

Computer-Assisted Design of Selective Imidazole Inhibitors for Cytochrome P450 Enzymes

Andreas Verras, Irwin D. Kuntz, and Paul R. Ortiz de Montellano*

Department of Pharmaceutical Chemistry, University of California, 600 16th Street, San Francisco, California 94143-2280

Received December 12, 2003

A modified version of the DOCK program has been used to predict inhibitors for cytochrome P450cam and its L244A mutant. A library ofazole compounds was designed in silico and screened for binding to wild-type P450cam. Lead compounds were synthesized and found to inhibit wild-type P450cam. To test our approach to designing ligands that discriminate between closely related sites, theazole library was DOCKed into both the active sites of wild-type P450cam and its L244A mutant. The L244A active site is predicted to be slightly larger than that of wild-type P450cam. Ligands predicted to have a high affinity for the mutant alone were synthesized and assayed with the recombinant enzymes. All of the compounds showed inhibition of the L244A enzyme ($IC_{50} = 6\text{--}40\ \mu\text{M}$), and the compounds that were predicted to be too large to bind to the wild-type showed poor inhibition ($IC_{50} \geq 1\ \text{mM}$). The binding mode was shown to be similar to that predicted by our modified version of DOCK by spectroscopic analysis. A discrepancy between the IC_{50} values and spectroscopic K_s values indicates that the spectroscopic binding constants do not accurately estimate inhibitory activity. This study, the first report of computer-assisted ligand (drug) design for P450 enzymes in which the coordination bond between imidazole and the heme is explicitly considered in structural modeling, opens a promising design avenue becauseazole compounds are widely used as P450 enzyme inhibitors and drugs.

Introduction

Cytochrome P450 enzymes, which catalyze the monooxygenation of a broad diversity of substrates, play essential roles in both the metabolism of xenobiotics and the biosynthesis and catabolism of endogenous lipophilic factors.¹ Inhibition of P450 enzymes, and therefore of the synthesis of endogenous factors, is a promising avenue for the development of therapeutic agents. Two examples are the inhibition of estradiol synthesis by aromatase in estrogen-dependent breast cancer and the possible control of retinoic acid levels through inhibition of P450-dependent retinoic acid metabolism.^{2,3} The inhibition of P450-dependent xenobiotic metabolism is also potentially desirable in situations in which xenobiotics are converted to toxic or carcinogenic metabolites.⁴ In a different context, the rapid selection of drug candidates that minimize the potential for P450-based drug–drug interactions is becoming increasingly important in the pharmaceutical industry.

Conventional drug design approaches have led to the development of a range of P450 inhibitors that are currently used in the clinic, primarily as antifungal agents. These agents include miconazole, ketoconazole, and fluconazole. It is likely that structure-based drug design methods will soon be applicable to the design of P450-targeted agents, as X-ray crystallography is beginning to yield structural information on relevant enzymes. In recent years, the structures of *Mycobacterium tuberculosis* sterol 14-demethylase, membrane-bound mammalian P450 enzymes, and even human P450 enzymes have been reported.^{5–7} With this influx of

structural data, computational methods that exploit this information and methods that are easily translatable across various P450 enzymes must be developed.

We report application of computational design methods for the generation of high-affinity inhibitors for cytochrome P450cam. To determine the ability of the approach to discriminate between closely related active sites, we have expressed the L244A mutant, which only differs from the parent enzyme by three carbon atoms, and then generated inhibitors that preferentially target the mutant. While P450cam is a bacterial enzyme of little interest as a drug target, it has been well characterized and represents an ideal system in which to test and refine the necessary approaches. The prediction of inhibitors for P450 enzymes presents a particular challenge because of the relatively low specificity of P450 active sites. In previous efforts, we have made some progress in predicting the substrate specificity of P450cam.⁸ However, this is the first instance in which such methods have been applied to the design of potential inhibitors of a structurally characterized P450 enzyme.

Results and Discussion

Virtual Library Design and a Modified DOCK-ing Algorithm. An initial virtual library of ligands was generated to screen for potential inhibitors for cytochrome P450cam. The choice of an imidazole scaffold was based on the knowledge that imidazoles and other aromatic nitrogen heterocycles that coordinate to the iron offer an effective route to inhibition of P450 enzymes.⁹ Past research into heme binding imidazoles indicates that substitution is limited to two positions.¹⁰ Thus, variation of the substituents at the 1 and 5

* To whom correspondence should be addressed. Phone: (415) 502-4728. Fax: (415) 502-4728. E-mail, ortiz@cgl.ucsf.edu.

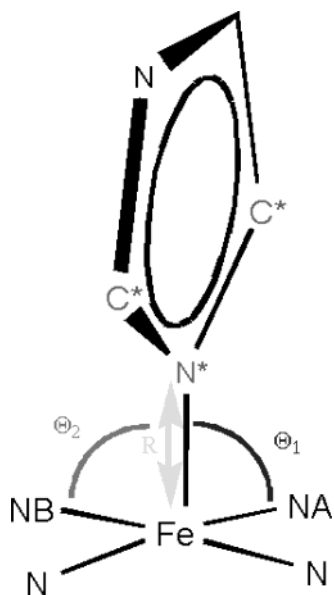


Figure 1. Covalent DOCK parameters. R is the distance from the heme iron to the imidazole N3. Θ_1 and Θ_2 are the angles as measured from nitrogens on the heme to the heme iron to imidazole N3. Light-faced atoms have their van der Waals contributions negated.

positions allows for the introduction of active site contacts and isoform specificity, whereas substitutions at the 2 or 4 positions introduce steric clashes with the heme moiety that preclude coordination of the imidazole to the heme iron atom. The nitrogen at position 3 of the imidazole must remain unsubstituted because it is the atom that actually coordinates to the iron (Figure 1). Substituents for the virtual library were taken from the ACD as described in the Experimental Section. A monosubstituted imidazole library was then constructed with the substituent exclusively in the 1N position because previous work suggested that a penalty exists for desolvating the unsubstituted 1N position.¹¹ However, the greatest library diversity was provided by the 1,5-disubstituted structures, which comprised 2550 of the total of 3508 structures.

Because DOCK does not recognize the coordinate imidazole–iron bond, initial attempts to DOCK the library produced unreasonable inhibitor orientations. Even when the ligand was preoriented correctly, the correct orientation was lost during minimization. To overcome this problem, Covalent DOCK (CovDOCK) was used. By introduction of a penalty for long imidazole N3–heme iron distances or improper angles, a binding mode was achieved that more correctly mimicked the binding observed in crystal structures of imidazole–P450 complexes (Figure 2). The binding of imidazole–P450 complexes diverges to some extent from any fixed distance and angle,^{11–13} so the harmonic restraints were deliberately set to low values to allow for this variation.

The best ligand among the initial hits had a CovDOCK score of -15.9 , compared to the value of -30 expected for a strong ligand hit. The relatively low scores, however, were not due to the harmonic penalties used in CovDOCK but were a consequence of the small active site and the lack of electrostatic interactions. It is also to be noted that the van der Waals' interactions of three imidazole atoms (C2, N3, and C4) are ignored in order to allow for a quasi-covalent imidazole–iron

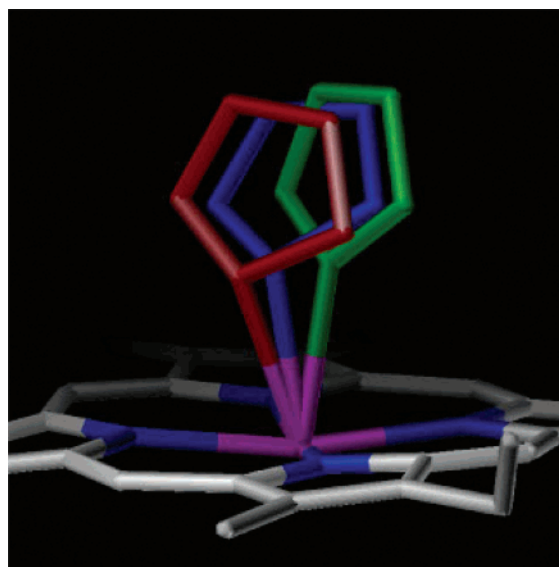


Figure 2. CovDOCK imidazole orientations, showing the number 1 (blue), 50 (green), and 150 (red) ranked compounds when CovDOCKed against wild-type P450cam. The side chains have been stripped to better illustrate the placement of the imidazole relative to the heme.

distance. This further decreases the effective size of the ligands and their overall CovDOCK score. A breakdown of the score contributions taken as absolute values to show their effective contributions to the overall CovDOCK score is illustrated in Figure 3. CovDOCK is able to return expected binding modes but does not dominate the score while doing so.

Inhibition of P450cam. As might be expected, the hits pulled from the library were primarily small ligands. The 200 top-scoring hits were clustered by Daylight fingerprints (Daylight Company, Santa Fe, NM), which effectively arranges them by functionality and not by 3D shape or conformation. A preference for monosubstituted imidazoles is immediately apparent in the preferred structure list despite the fact that monosubstituted ligands represent less than one-third of the total virtual library. Representatives of several attractive clusters from among the top 200 ranked ligands were selected for experimental evaluation and were synthesized. Ligands were chosen for synthesis by manually inspecting the top 200 ranked compounds and selecting ligands that had good binding modes and maintained an imidazole–heme coordinate character similar to that found in the crystallographic data. The ability of the compounds to inhibit the oxidation of camphor to 5-*exo*-hydroxycamphor was measured by gas chromatographic analysis of the product to starting material ratio. All of the monosubstituted compounds showed good inhibition of wild-type P450cam; most were in the low micromolar range (Table 1). The monosubstituted compounds were then assayed against the L244A mutant, and the results, as expected, indicated a preference for the wild-type. The results are shown on a log scale to better illustrate the differences in inhibitory activity between the wild-type and mutant (Figure 4). There is more space created by the L244A mutation that is not exploited by the monosubstituted compounds. While being able to generate high-affinity inhibitors in a first round synthesis is promising in

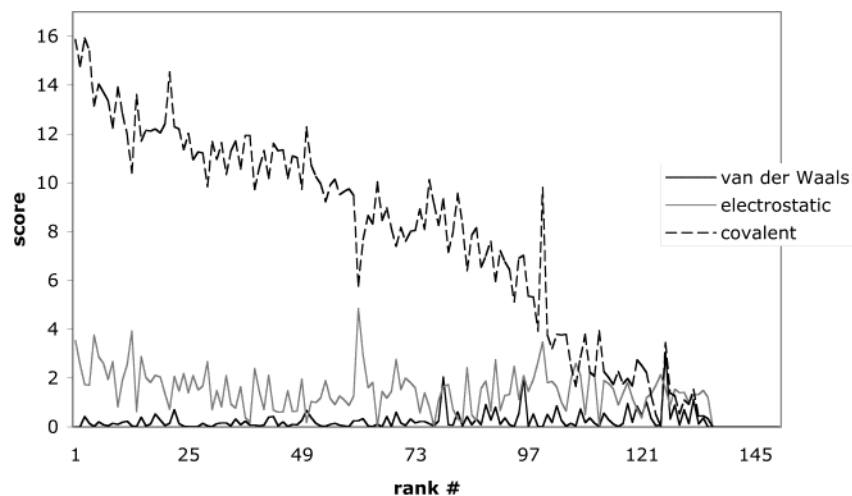


Figure 3. Covalent DOCK score breakdown indicated by Covalent DOCK score contribution to the overall DOCK score. The absolute values of the score components are displayed to show relative magnitude.

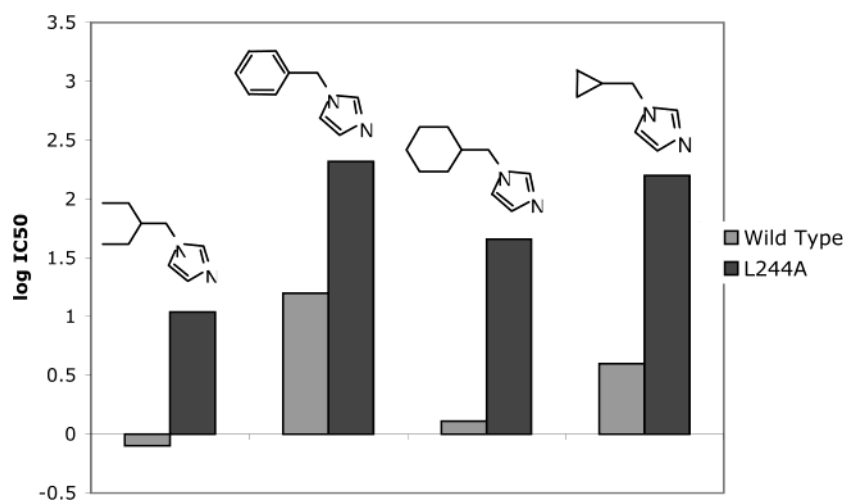
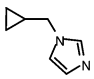
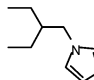
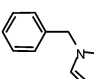
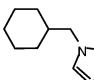


Figure 4. Monosubstituted IC_{50} selectivity indicated by monosubstituted compound IC_{50} values assayed against the wild-type and the L244A mutant.

Table 1. Monosubstituted IC_{50} Values and CovDOCK Scores^a

	IC_{50} μM	CovDOCK scores
	4 ± 2.0	-6.23
	$0.8 \pm .3$	-2.48
	16 ± 11	-6.97
	$1.5 \pm .5$	-9.51

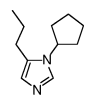
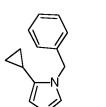
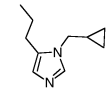
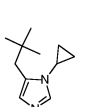
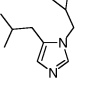
^a Monosubstituted ligands synthesized and their IC_{50} values and CovDOCK scores against wild-type P450cam.

itself, we were particularly interested in generating compounds selective for the L244A mutant by rational design.

We used CovDOCK to search for inhibitors predicted to exhibit a high affinity for the L244A mutant and, simultaneously, a mitigated affinity for wild-type

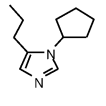
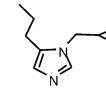
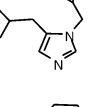
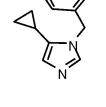
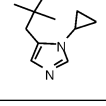
P450cam. The L244A mutation was made in the 1PHD PDB structure using Sybyl, and a grid was generated for CovDOCKing without minimization. The original virtual library was then covalently DOCKed into this L244A active site. In an effort to generate selective inhibitors, the best hits against the mutant were taken and CovDOCKed into wild-type P450cam. Large differences in the CovDOCK score (>50) were assumed to represent active site clashes and thus a potential poor fit. By comparing the CovDOCK results between the two active sites, we hoped to find the characteristics of ligands that would inhibit the L244A isozyme selectively. Gschwend and Kuntz¹⁴ used a similar approach before, predicting selectivity by computational screening between two strains of dihydrofolate reductase. Table 2 illustrates the scores for several of our compounds against the L244A mutant and the differences between the scores for the two forms of the enzyme. A major difference between compounds predicted to be inhibitors for the L244A vs the wild-type is quickly apparent in the second substituent on the imidazole at the 5 position. While these disubstituted compounds comprise two-thirds of the library, they were not predicted to fit into the wild-type, and when they were redocked into the wild-type, they were found to have high scores due

Table 2. Second-Round CovDOCK Results^a

Chemical Structure	RANK	Score Diff.	Chemical Structure	RANK	Score Diff.
	216	-195.1		195	-10.22
	57	-47.18		25	-73.15
	29	-49.99			

^a Disubstituted compounds rank against the L244A mutant as scored by CovDOCK and the difference in score when the same compound is covalently DOCKed back into the wild-type enzyme.

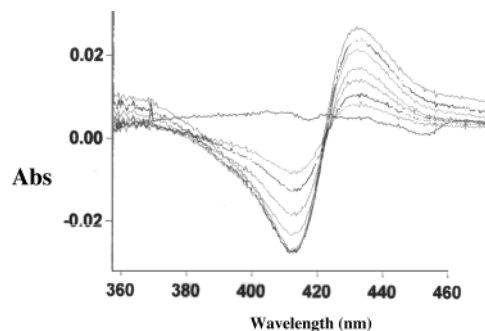
Table 3. Disubstituted IC₅₀ Values^a

Chemical Structure	L244A IC ₅₀ (μM)	WTYP E %Inhibition at 1mM
	6.5 ± .4	60
	36 ± 7	60
	10.1 ± .5	20
	41 ± 6	30
	129 ± 45	80

^a Disubstituted compounds synthesized and their inhibition of L244A and wild-type P450cam enzymes.

to steric clashes. Notably, the second substituent on the ligands predicted to bind to the L244A is generally small, in agreement with the small active site change due to mutating a leucine to an alanine. On the basis of these results, the disubstituted compounds were predicted to be selective inhibitors and five ligands were chosen for synthesis. The criteria for selection included good imidazole–heme coordination, a good CovDOCK score against the L244A mutant, and a poor score against the wild-type.

The disubstituted compounds, as predicted, have good affinity for the L244A protein (Table 3). When assayed against the wild-type, they show almost no inhibition, and even at a 1 mM concentration none of the disubstituted compounds completely inhibited catalytic activity. These results are very promising because they suggest that we were able to predictively identify ligands complementary to the L244A active site but slightly too large to be able to inhibit the wild-type.

**Figure 5.** Difference spectrum of 1-cyclopentyl-5-propylimidazole. This type II shift is seen with all the inhibitors.

Spectroscopic Analysis. Binding of the compounds was evaluated spectrophotometrically. To ensure a similar starting state, a difference spectrum was taken in which inhibitors were titrated into solution in the absence of camphor. All of the inhibitors exhibited a type II spectral shift in which the water-coordinated Soret maximum at 417 nm disappeared while the 424 nm imidazole-bound peak intensified. This shift is consistent with binding of a primary or aromatic nitrogen as the sixth ligand to the iron.¹⁵ Figure 5, which illustrates the difference spectra obtained with 1-cyclopentyl-5-propylimidazole, is typical of all of the spectra used to determine the K_s values. A clear isosbestic point is observed, and the transition to 424 nm is saturatable. The spectroscopic data agree with the binding mode predicted by CovDOCK.

The L244A P450cam is very similar to wild-type P450cam spectroscopically: both have a 450 nm peak in the reduced CO-bound state, and both enzymes absorb in the ferric state at the same wavelength, both in the high spin (390 nm, no sixth ligand) and low spin (416 nm, water-coordinated) states. Furthermore, the affinity for camphor, the natural substrate, remains unchanged (wild-type $K_s = 1.3 \pm 0.2 \mu\text{M}$, L244A $K_s = 1.5 \pm 0.2 \mu\text{M}$). The L244A mutant, as previously reported, is catalytically viable and, though it turns over camphor more slowly, exhibits a degree of uncoupling nearly identical to that of the wild-type enzyme.¹⁶ This means that the NADH and O₂ consumed by the enzyme are used to the same extent in hydroxylation of camphor rather than in the production of H₂O₂ or H₂O. Nevertheless, an important difference was found in the affinity of the two forms of the enzyme for imidazole. The K_s of wild-type P450cam for unsubstituted imidazole is $7.5 \pm 1.4 \mu\text{M}$, whereas that of the L244A mutant is $304 \pm 49 \mu\text{M}$. This 43-fold difference was unexpected because the spectroscopic, substrate binding, catalytic, and uncoupling data suggest that the wild-type and mutant active sites are very similar. The loss of affinity for imidazole presumably reflects active site changes such as an increase in the active site water content, possible changes in the positioning of water molecules, and small perturbations of active site residues that do not alter the protein spectrum or its natural affinity for camphor. Reports of azole resistance among fungal strains are increasing,^{17,18} and the L244A mutant may provide a useful model in this regard. Furthermore, the data indicate that our disubstituted inhibitors are able to compensate for the imidazole scaffold's mitigated affinity for the L244A active site.

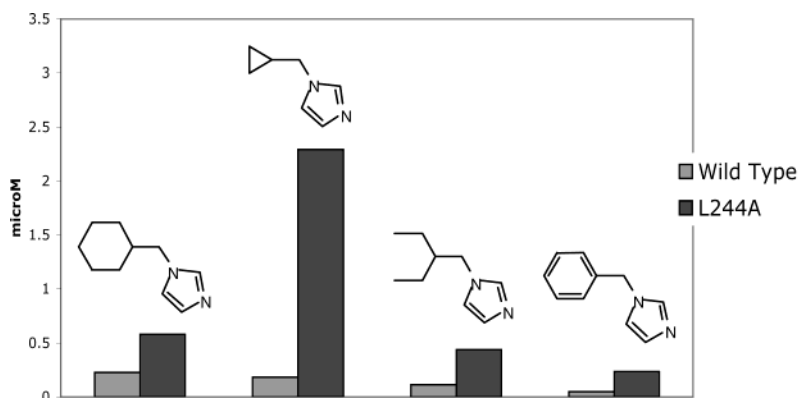


Figure 6. Monosubstituted compound K_s values against wild-type P450cam and its L244A mutant.

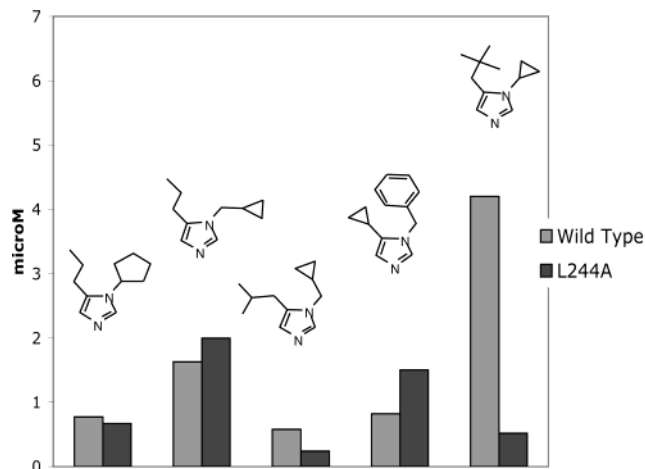
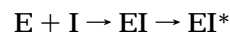


Figure 7. Disubstituted compound K_s values against wild-type P450cam and its L244A mutant.

The K_s values for the monosubstituted compounds against both the L244A and wild-type P450 enzymes are shown in Figure 6. A general trend toward selectivity is evident and expected given the difference in base affinities of the scaffolds. Surprisingly, the K_s values for the disubstituted compounds do not reflect the high selectivity observed in the IC_{50} assays (Figure 7). While the IC_{50} assays are done in the presence of camphor (250 μ M), it is still surprising that such a large discrepancy exists. In theory, if the disubstituted compounds are able to coordinate to the iron, they should prevent electron transfer and catalysis; however, even at inhibitor concentrations up to 1 mM, activity is still seen in the presence of the disubstituted ligands.

While exploration of the intricacies of this anomaly is outside the scope of this paper, it is clear that this observation is related to a requirement of conformational changes in the P450cam active site. Support for this argument is provided by measurements of K_s values of ligands predicted to be too large to fit into either active site. Thus, 1,5-dicyclohexylimidazole binds to both the wild-type (90 ± 55) and the L244A mutant (20 ± 4) even though, on the basis of a rigid model of the protein, this large, disubstituted compound should be unable to bind to either the wild-type or L244A active site. Even more surprisingly ketoconazole was found to bind with high affinity to both the wild-type (0.5 ± 0.1) and L244A mutant (0.6 ± 0.1). No crystal structure of P450cam exists that suggests an active site anywhere large enough to accommodate this ligand. Thus, a conformational change must occur.

The exact nature of the conformational changes, and the reason for the low inhibitory activity of some compounds that have low spectroscopic binding constants (K_s values), remain to be defined. One possibility is that the large inhibitors require a slow conformational change and are thus slow-binding, reversible inhibitors that adhere to the following kinetic model:¹⁹



However, we have not observed the time dependence in the K_s value determinations implied by this model. Thus, although conformational changes are clearly involved in the discrepancy between the K_s and IC_{50} values, the definition of the precise relationship between these values requires further exploration.

Conclusions

We have shown that it is possible, using structure-based design and currently available docking algorithms, to generate ligands of high affinity for both cytochrome P450cam and, more importantly, its L244A mutant. The CovDOCK method and azole libraries offer promise as a facile, modular system easily applicable to crystallographically characterized P450 enzymes. The library construction was based on synthetic feasibility and is not limited to the 3500 compounds actually included in this study. Indeed, the library has recently been expanded to 4500 compounds and is completely amenable to the inclusion of alternative P450-coordinating scaffolds such as triazoles, pyridines, and other heterocycles, all of which would significantly increase the chemical diversity of the library.

On the basis of the IC_{50} data, we were able to exploit small differences in the active sites of these two isozymes and synthesize two distinct groups of ligands with selectivity for either enzyme. The results are promising, and with the accelerating pace of determination of P450 crystal structures and the swift screening methods made possible by computational advances, one can envision that dozens, even scores, of enzymes could be DOCKed in an effort to generate isoform selectivity.

Although P450cam can hydroxylate a variety of non-natural substrates,¹⁵ the enzyme has a single natural substrate (camphor) and has clearly evolved to optimize its oxidation. P450cam has generally been thought to have a relatively rigid active site because crystal structures of the enzyme with various substrates and inhibitors show only minor adjustments of the active

site cavity.^{11,20,21} Of course, it is evident that the protein must undergo substantial conformational changes to allow the entry of substrates into the active site cavity because no entry channel is seen in the crystal structure. The spectroscopic results demonstrate that conformational mobility, even in an enzyme such as P450cam, is an important parameter in identifying ligands that differentiate between two similar P450 active sites. Also, while spectroscopic assays are frequently the initial test of binding to cytochrome P450 enzymes, our results suggest that they can be misleading in inhibitor prediction. Studies measuring spectroscopic binding to microsomal P450 enzymes and in vivo activity have shown discrepancies between K_s and IC_{50} values.²² Our results suggest that discrepancies may also exist in single enzyme studies and that caution must be employed when screening ligands for inhibitory potential by spectroscopic means.

Experimental Section

Protein Expression and Binding Assays. Cytochrome P450cam and the P450cam L244A mutant were expressed in *Escherichia coli* as previously reported.²³ Both proteins were stored with 100 μ M camphor at -70 °C. Camphor was removed before the proteins were used by twice eluting with 100 mM sodium phosphate through a PD-10 size exclusion column. The P450cam thus obtained has a water coordinated to the heme iron and is in the low-spin state. Spectroscopic binding (K_s) assays were done in 100 mM potassium phosphate buffer at 37 °C by difference UV spectroscopy. The two cuvettes contained 0.5 μ M protein in 300 μ L of 100 mM potassium phosphate buffer. The potential inhibitors were dissolved in DMSO with the exception of imidazole, which was dissolved in water. DMSO never constituted more than 2% of the final sample volume. An equal amount of DMSO was added to the reference cuvette, and the shift in absorbance from 416 to 424 nm as increasing concentrations of camphor were titrated into the cuvette was observed. The difference between 416 and 424 nm values was then recorded and fitted to a binding curve to obtain K_s values. K_s values were calculated by nonlinear regression analysis using the equation

$$\Delta A = \frac{\Delta A_{\max} [I]}{K_s + [I]}$$

where ΔA is the 416 trough to 424 peak absorbance difference, ΔA_{\max} is the difference in absorption at saturation, and $[I]$ is the inhibitor or ligand concentration.²⁴

The compounds reported in this study were synthesized except for imidazole, 1,5-dicyclohexylimidazole, and ketoconazole. Imidazole and 1,5-dicyclohexylimidazole were purchased from Aldrich (St. Louis, MO), and ketoconazole was obtained from Jansen Pharmaceuticals (Beerse, Belgium).

Gas Chromatographic Inhibition Assay and IC_{50} Calculation. Catalytic activity was quantitated by gas chromatographic product analysis. The protein was eluted twice through a PD-10 column with 100 mM sodium phosphate to remove camphor. Assays were done under the following conditions: P450cam 5 nM, putidaredoxin 2 μ M, putidaredoxin reductase 2 μ M, camphor 250 μ M, and NADH 1000 μ M. The L244A protein was assayed at a concentration of 20 nM. The total reaction volume was 150 μ L. Varying amounts of inhibitor were added in DMSO, but the DMSO volume never exceeded 3% of the total reaction volume. All assays were done in 100 mM potassium phosphate in a 20 °C bath for 15 min. The reactions were then quenched with 20 μ L of CH_2Cl_2 containing 2 mM β -thujone as an internal standard.

The CH_2Cl_2 was then withdrawn directly from the reaction mixture and injected onto an HP 5980 series II gas chromatograph equipped with an Agilent Technologies (Palo Alto, CA) DB-10 capillary column. A temperature gradient from 40 to

280 °C over 20 min was used. The β -thujone standard eluted at approximately 6 min, starting material eluted at approximately 6.2 min, and product appeared at 9.9 min. The difference between the product to starting material ratio was then used to calculate turnover. IC_{50} values were calculated by the Langmuir isotherm equation:²⁵

$$\text{Activity} = 1 + \left(1 + \frac{IC_{50}}{[Inh]} \right)$$

Organic Synthesis. Two rounds of synthesis were done. Initially all the imidazoles synthesized were N-monoalkylated and were prepared as previously reported.²⁶ The syntheses of N-benzylimidazole and N-cyclopropylmethylimidazole are described here as typical procedures.

N-Benzylimidazole. Imidazole (100 mg, 1.4 mmol) was suspended in 5 mL of acetone under argon in a round-bottom flask. Dry, powdered KOH (392.7 mg, 7 mmol) was added with stirring. The solution became beige. After 3 min a 190 μ L aliquot of benzyl bromide (1.57 mmol) was added dropwise, and a white precipitate appeared. The acetone was removed on a rotary evaporator, and the precipitate was resuspended in CH_2Cl_2 . Water was added, the solution pH was lowered to ~ 4 with concentrated HCl, and the product was extracted in the aqueous layer. The pH of the aqueous layer was then raised to ~ 10 with concentrated NaOH, and the product was extracted with CH_2Cl_2 and crystallized directly from CH_2Cl_2 . The purity and identity were judged by TLC (ethyl acetate + 1% triethylamine, $R_f = 0.1$), mass spectrometry, and NMR: 17% yield; mp 73–74 °C (reported 72–74 °C); 1H NMR ($CDCl_3$) δ 7.52 (1H, s, imidazole), 7.08 (1H, s, imidazole), 6.88 (1H, s, imidazole), 5.18 (2H, s, NCH_2), 7.14 benzyl (2H, d, aryl, $J = 8.0$ Hz), 7.33 (2H, m, aryl), and 7.32 (1H, m, aryl); ^{13}C NMR (DMSO) δ 137.4, 136.18, 129.83, 128.99, 128.27, 127.28, and 50.8; EI-MS, m/z (low resolu), 159.25 (M + H).

1-Methylcyclopropylimidazole. Imidazole (100 mg, 1.4 mmol) was suspended and deprotonated as described above. A 230 μ L aliquot of bromomethylcyclopropane (1.57 mmol) was added dropwise, and the solution became a darker shade of beige. The reaction was worked up as described above and, after an acid–base wash, the solution was concentrated by rotary evaporation to give a yellow oil that was deemed sufficiently pure by TLC (ethyl acetate + 1% triethylamine, $R_f = 0.1$), mass spectrometry, and NMR for direct study: 50% yield; 1H NMR ($CDCl_3$) δ 7.55 (1H, s, imidazole), 7.06 (1H, s, imidazole), 6.99 (1H, s, imidazole), 3.79 (2H, d, NCH_2 , $J = 6.8$ Hz), 1.2 (1H, m, cyclopropyl), 0.68 ppm (2H, q, cyclopropyl, $J = 8.0$ Hz), and 0.36 (2H, q, cyclopropyl, $J = 4.2$ Hz); ^{13}C NMR (DMSO) δ 137.37, 128.62, 119.75, 50.85, 12.58, 4.08; EI-MS, m/z , exptl 122.0843 (M^+) (calcd 122.0844, $C_7H_{10}N_2$).

The second round of ligands prepared as potential inhibitors of the P450cam L244A mutant were all 1,5-disubstituted compounds. These were prepared by a two-step synthesis utilizing the synthon tosylmethyl isocyanide.²⁷ The yields were generally low, less than 10%, but the reactions afforded sufficient product for the spectroscopic and kinetic assays. The synthesis of 1-benzyl-5-cyclopropylimidazole is given as a typical procedure.

1-Benzyl-5-cyclopropylimidazole. To ~ 2 mL of dry molecular sieves was added 10 mL of anhydrous CH_2Cl_2 , followed by benzylamine (1.46 mL, 13.1 mmol) and subsequently by dropwise addition of cyclopropylcarboxaldehyde (1 mL, 13.1 mmol). The disappearance of the aldehyde peak and appearance of the imine peak were monitored by infrared spectroscopy. After 2 h, the reaction mixture was filtered and rotary-evaporated to give a clear-yellow product that was used as obtained in the following step.

Dry potassium carbonate (9.55 g, 50 mmol) was added to tosylmethyl isocyanide (1.99 g, 10 mmol) suspended in 15 mL of anhydrous MeOH followed by dropwise addition of the imine product from the previous reaction. The resulting solution was allowed to stir for 24 h and was then filtered, the filtrate was subjected to rotary evaporation, and the residue was extracted thrice with ether (3×20 mL). The product was purified by

flash chromatography on silica with a solvent system consisting initially of 300 mL of 50/50 (v/v) of hexane/ethyl acetate followed by 80/20 (v/v) of ethyl acetate/methanol. The desired product is one of the final substances to be eluted because of the protonated imidazole nitrogen. Finally, the product was partitioned between acid and base as described above. Rotary evaporation of the solution then yielded a yellow oil that was pure by TLC (ethyl acetate/methanol 80/20, $R_f = 0.2$) and NMR.

The following compounds were made by the appropriate procedure described above.

1-Methylcyclohexylimidazole: 22% yield; ^1H NMR (CDCl_3) δ 7.34 (1H, s, imidazole), 6.97 (1H, s, imidazole), 6.79 (1H, s, imidazole), 3.65 (2H, d, NCH_2 , $J = 8.2$ Hz), 1.5–1.7 ppm (6H, m, cyclohexyl), and 1.05–1.19 (5H, m, cyclohexyl); ^{13}C NMR (DMSO) δ 137.83, 128.11, 119.80, 52.01, 36.10, 29.82, 25.86, 25.09; EI-MS, m/z exptl 164.1313 (M^+) (calcd 164.1313, $\text{C}_{10}\text{H}_{16}\text{N}_2$).

1-(2-Ethylbutyl)imidazole: 56% yield; ^1H NMR (CDCl_3) δ 7.42 (1H, s, imidazole), 7.03 (1H, s, imidazole), 6.85 (1H, s, imidazole), 3.81 (2H, d, NCH_2 , $J = 8$ Hz), 1.63 (1H, septuplet, 2-ethylbutyl), 1.27 (4H, pentuplet, 2-ethylbutyl, $J = 9.4$ Hz), and 0.87 (6H, t, $t\text{-CH}_3$, $J = 8.2$ Hz); ^{13}C NMR (DMSO) δ 137.63, 128.13, 119.71, 49.04, 36.10, 22.57, 10.34; EI-MS, m/z exptl 152.1338 (M^+) (calcd 152.1313, $\text{C}_9\text{H}_{16}\text{N}_2$).

1-Cyclopentyl-5-propylimidazole: 3% yield; ^1H NMR (CDCl_3) δ 7.49 (1H, s, imidazole), 6.79 (1H, s, imidazole), 4.33 (1H, pentuplet, cyclopentyl, $J = 8.0$ Hz), 2.52 (2H, t, propyl, $J = 8.0$ Hz), 1.6–1.95 (10H, m), and 1.05 (3H, t, propyl, $J = 7.2$ Hz); ^{13}C NMR (CDCl_3) 133.58, 131.72, 125.5, 55.72, 33.47, 26.27, 23.76, 21.45, 13.8; EI-MS, m/z exptl 178.1469 (M^+) (calcd 178.1470, $\text{C}_{11}\text{H}_{18}\text{N}_2$).

1-Methylcyclopropyl-5-propylimidazole: 11% yield; ^1H NMR (CDCl_3) δ 7.65 (1H, s, imidazole), 6.77 (1H, s, imidazole), 3.62 (2H, d, NCH_2 , $J = 6.8$ Hz), 2.53 (2H, t, propyl, $J = 8.0$ Hz), 1.76 (2H, sextet, propyl, $J = 7.2$ Hz), 1.21 (1H, m, cyclopropyl), 0.98 (3H, t, propyl, $J = 7.2$ Hz), 0.34 (2H, q, cyclopropyl, $J = 5.2$ Hz), and 0.24 (2H, q, cyclopropyl, $J = 4.4$ Hz); ^{13}C NMR (CDCl_3) δ 136.07, 132.62, 125.70, 49.46, 23.46, 19.27, 14.16, 10.91, 4.14; EI-MS, m/z exptl 164.1313 (M^+) (calcd 164.1313, $\text{C}_{10}\text{H}_{16}\text{N}_2$).

1-Methylcyclopropyl-5-butylimidazole: 13% yield; ^1H NMR (CDCl_3) δ 7.53 (1H, s, imidazole), 6.77 (1H, s, imidazole), 3.66 (2H, d, NCH_2 , $J = 6.8$ Hz), 2.41 (2H, d, butyl, $J = 7.2$ Hz), 1.88 (1H, nonatet, butyl, $J = 6.8$ Hz), 1.16 (1H, m, cyclopropyl), 0.66 (2H, q, cyclopropyl, $J = 8.4$ Hz), and 0.33 (2H, q, cyclopropyl, $J = 4.8$ Hz); ^{13}C NMR (CDCl_3) δ 136.01, 130.32, 126.66, 49.04, 32.97, 27.81, 22.32, 11.12, 4.08; EI-MS, m/z exptl 178.1470 (M^+) (calcd 178.1470, $\text{C}_{11}\text{H}_{18}\text{N}_2$).

1-Benzyl-5-cyclopropylimidazole: 6% yield; ^1H NMR (CDCl_3) δ 7.42 (1H, s, imidazole), 6.84 (1H, s, imidazole), 5.15 (2H, s, methyl), 7.23–7.34 (5H, m, benzyl), 0.91 (1H, m, cyclopropyl), 0.85 (2H, m, cyclopropyl), and 0.68 (2H, q, cyclopropyl, $J = 4.4$); ^{13}C NMR (CDCl_3) δ 137.161, 136.44, 134.24, 128.70, 128.40, 127.74, 125.72, 48.31, 5.51, 4.34; EI-MS, m/z exptl 198.1153 (M^+) (calcd 198.1157, $\text{C}_{13}\text{H}_{14}\text{N}_2$).

1-Cyclopropyl-5-tert-butylimidazole: 9% yield; ^1H NMR (CDCl_3) δ 7.41 (1H, s, imidazole), 6.77 (1H, s, imidazole), 3.09 (1H, m, cyclopropyl), 2.13 (2H, s, tert-butyl), 1.0 (9H, s, tert-butyl CH_3), and 0.85–1.05 (4H, m, cyclopropyl); ^{13}C NMR (CDCl_3) δ 136.54, 129.62, 127.87, 37.20, 30.78, 29.32, 26.04, 6.25; EI-MS, m/z exptl 178.1467 (M^+) (calcd 178.1470, $\text{C}_{11}\text{H}_{18}\text{N}_2$).

Library Design. Because azole compounds have long been known for their utility as P450 inhibitors,⁹ we chose an imidazole scaffold for this project. To create the virtual library, the imidazole scaffold was modeled in SYBYL (Tripos Inc., St. Louis, MO) and substituents were selected from the Available Chemical Database (ACD) (Molecular Design Systems, San Leandro, CA) based on potential synthetic routes for creating 1-alkylimidazoles,²⁶ 1-arylimidazoles,²⁸ and 1,5-disubstituted imidazoles.²⁷ The corresponding primary and secondary halide, aniline, aldehyde, and primary amine reactants were extracted from the ACD using Merlin (Daylight Company, Santa Fe, NM) and UCSelect (G. Skillman, Ph.D. thesis, UCSF). Our

primary criterion for reactant selection was synthetic feasibility. A virtual library of 582 primary and secondary alkyl halides, 378 anilines, 51 aldehydes, and 50 primary amines was compiled. The fragments were joined to their appropriate position on the imidazole scaffold using SYBYL. The final library contained 3508 compounds: 479 N-alkylated imidazoles, 376 N-arylimidazoles, and 2550 1,5-disubstituted imidazoles.

Covalent DOCK. DOCK 4.0²⁹ was employed to screen the library against cytochrome P450cam. Grid coordinates were taken from the 1PHD imidazole complexed structure determined by Poulos.¹¹ The charges for the heme were taken from the semiempirical ZINDO calculations of Gilda Loew.³⁰

Covalent DOCK (CovDOCK) (G. Skillman, Ph.D. thesis, UCSF), originally written to apply to serine proteases, was modified to model the imidazole–iron coordinate bond. CovDOCK adds harmonic restraints to the DOCK scoring function:

$$\begin{aligned} \text{CovDOCK score} &= k_1(\text{dist})^2 + \\ & k_2(\text{angle A})^2 + k_3(\text{angle B})^2 \quad (1) \\ k_1 &= 50; k_2 = 0.01; k_3 = 0.01 \end{aligned}$$

The three restraints used in this work were a distance restraint from the iron to the imidazole N3 and two orthogonal angle restraints from nitrogens NA and NB on the heme to the iron and to the imidazole N3 (Figure 1). The van der Waals contributions of the nitrogen coordinating the imidazole to the heme as well as the carbons adjacent to the heme were set to zero. Removing the van der Waals contributions of these atoms was necessary to allow for the close contacts observed in crystal structures of P450 imidazole inhibitor complexes.

Acknowledgment. We thank Wesley Straub for help with the synthetic organic chemistry procedures, Geoffrey Skillman for advice and the use of his code, and Susan Miller for discussions of inhibitor kinetics. This work was supported by National Institutes of Health Grants GM25515 and GM56531 and by a BioStar grant from California.

References

- Ortiz de Montellano, P. R. In *Cytochrome P450: Structure, Mechanism, and Biochemistry*, 2nd ed.; Ortiz de Montellano, P. R., Ed.; Plenum Press: New York, 1995.
- Guengerich, P.; Chun, Y.; Kim, D.; Gillam, E.; Shimada, T. Cytochrome P450 1B1: a target for inhibition in anticarcinogenesis strategies. *Mutat. Res./Fundam. Mol. Mech. Mutagen.* **2003**, *523*, 173–182.
- Fujii, H.; Sato, T.; Kaneko, S.; Gotoh, O.; Fujii-Kuriyama, Y.; Osawa, K.; Kato, S.; Hamada, H. Metabolic inactivation of retinoic acid by a novel P450 differentially expressed in developing mouse embryos. *EMBO J.* **1997**, *16*, 4163–4173.
- McLemore, T. L.; Litterst, C. L.; Coudert, B. P.; Liu, M. C.; Hubbard, W. C.; Adelberg, S.; Czerwinski, M.; McMahon, J. A.; Eggleston, J. C.; Boyd, M. R. Metabolic activation of 4-ipomeanol in human lung, primary pulmonary carcinomas, and established human pulmonary carcinoma cell lines. *J. Nat. Cancer Inst.* **1990**, *82*, 1420–1426.
- Podust, L. M.; Stojan, J.; Poulos, T. L.; Waterman, M. R. Substrate recognition sites in 14-sterol demethylase from comparative analysis of amino acid sequences and X-ray structure of *Mycobacterium tuberculosis* CYP51. *J. Inorg. Biochem.* **2001**, *87*, 227–235.
- Williams, P. A.; Cosme, J.; Sridhar, V.; Johnson, E. F.; McRee, D. E. Mammalian microsomal cytochrome P450 monooxygenase: structural adaptations for membrane binding and functional diversity. *Mol. Cell* **2000**, *5*, 121–131.
- Williams, P. A.; Cosme, J.; Ward, A.; Angove, H. C.; Vinkovi, D. M.; Jhoti, H. Crystal structure of human cytochrome P450 2C9 with bound warfarin. *Nature* **2003**, *424*, 464–468.
- Zhang, Z.; Sibbesen, O.; Johnson, R. A.; Ortiz de Montellano, P. R. The substrate specificity of cytochrome P450cam. *Bioorg. Med. Chem.* **1988**, *6*, 1501–1508.
- Testa, B.; Jenner, P. Inhibitors of cytochrome P-450s and their mechanism of action. *Drug Metab. Rev.* **1981**, *12*, 1–117.

- (10) Rogerson, T. D.; Wilkinson, C. F.; Hetarski, K. Steric factors in the inhibitory interaction of imidazoles with microsomal enzymes. *Biochem. Pharmacol.* **1977**, *26*, 1039–1042.
- (11) Poulos, T. L.; Howard, A. J. Crystal structures of metyrapone and phenylimidazole-inhibited complexes of cytochrome P-450cam. *Biochemistry* **1987**, *26*, 8165–8174.
- (12) Yano, J. K.; Koo, L. S.; Schuller, D. J.; Li, H.; Ortiz de Montellano, P. R.; Poulos, T. L. Crystal structure of a thermophilic cytochrome P450 from the archaeon *Sulfolobus solfataricus*. *J. Biol. Chem.* **2000**, *275*, 31086–31092.
- (13) Podust, L. M.; Poulos, T. L.; Waterman, M. R. Crystal Structure of cytochrome P450 14 α -sterol demethylase (Cyp51) from *Mycobacterium tuberculosis* in complex with azole inhibitors. *Proc. Natl. Acad. Sci. U.S.A.* **2001**, *98*, 3068–3073.
- (14) Gschwend, D. A.; Sirawaraporn, W.; Santi, D. V.; Kuntz, I. D. Specificity in structure-based drug design: identification of a novel, selective inhibitor of *Pneumocystis carinii* dihydrofolate reductase. *Proteins* **1997**, *29*, 59–67.
- (15) Schenkman, J. B.; Remmer, H.; Estabrook, R. W. Spectral studies of drug interaction with hepatic microsomal cytochrome. *Mol. Pharmacol.* **1967**, *3*, 113–123.
- (16) De Voss, J. J.; Sibbesen, O.; Zhang, Z. P.; Ortiz de Montellano, P. R. Substrate docking algorithms and prediction of the substrate specificity of cytochrome P450cam and its L244A mutant. *J. Am. Chem. Soc.* **1997**, *119*, 5489–5498.
- (17) Kelly, S. L.; Lamb, D. C.; Cannieux, M.; Greetham, D.; Jackson, C. J.; Marczylo, T.; Ugochukwu, C.; Kelly, D. E. An old activity in the cytochrome P450 superfamily (CYP51) and a new story of drugs and resistance. *Biochem. Soc. Trans.* **2001**, *29*, 122–128.
- (18) Kelly, S. L.; Lamb, D. C.; Loeffler, J.; Einsele, H.; Kelly, D. E. The G464S amino acid substitution in *Candida albicans* sterol 14 α -demethylase causes fluconazole resistance in the clinic through reduced affinity. *Biochem. Biophys. Res. Commun.* **1999**, *262*, 174–179.
- (19) Morrison, J. F.; Walsh, C. T. The behavior and significance of slow-binding enzyme inhibitors. *Adv. Enzymol. Relat. Areas Mol. Biol.* **1988**, *61*, 201–301.
- (20) Poulos, T. L.; Finzel, B. C.; Howard, A. J. High-resolution crystal structure of cytochrome P450cam. *J. Mol. Biol.* **1987**, *195*, 687–700.
- (21) Raag, R.; Poulos, T. L. Crystal structures of cytochrome P-450cam complexed with camphane, thiocamphor, and adamantane: factors controlling P-450 substrate hydroxylation. *Biochemistry* **1991**, *30*, 2674–2684.
- (22) Lavrijsen, K.; Houdt, J. V.; Thijs, D.; Meuldrmans, W.; Heykants, J. Induction potential of antifungals containing an imidazole or triazole moiety. Miconazole and ketoconazole, but not itraconazole are able to induce hepatic drug metabolizing enzymes of male rats at high doses. *Biochem. Pharmacol.* **1986**, *35*, 1867–1878.
- (23) Gunsalus, I. C.; Wagner, G. C. In *Methods in Enzymology*; Fleischer, S., Packer, L., Eds.; Academic Press: New York, 1978; Vol. 52, Part C, pp 166–188.
- (24) Rao, S.; Wilks, A.; Hamberg, M.; Ortiz de Montellano, P. R. The lipoxygenase activity of myoglobin. Oxidation of linoleic acid by the ferryl oxygen rather than protein radical. *J. Biol. Chem.* **1994**, *269*, 7210–7216.
- (25) Copeland, R. A. *Enzymes*, 2nd ed.; Wiley-VCH: New York, 2000; pp 76–109.
- (26) Grimmett, M. R. *Comprehensive Heterocyclic Chemistry*; Katritzky, A. R., Rees, Ch. W., Eds.; Pergamon Press: Oxford, 1984; p 382.
- (27) Leusen, A.; Wildeman, J.; Oldenziel, O. Base-induced cycloaddition of sulfonylethyl isocyanides to C,N double bonds. Synthesis of 1,5-disubstituted and 1,4,5-trisubstituted imidazoles from aldimines and imidoyle chlorides. *J. Org. Chem.* **1977**, *42*, 1153–1159.
- (28) Johnson, A. L.; Kauer, D.; Sharma, D. C.; Dorfman, R. I. The synthesis of 1-arylimidazoles, a new class of steroid hydroxylation inhibitors. *J. Med. Chem.* **1969**, *12*, 1024–1028.
- (29) Ewing, T. J.; Makino, S.; Skillman, A. G.; Kuntz, I. D. DOCK 4.0: search strategies for automated molecular docking of flexible molecule databases. *J. Comput.-Aided Mol. Des.* **2001**, *15*, 411–428.
- (30) Collins, J. R.; Camper, D. L.; Loew, G. H. Valproic acid metabolism by cytochrome P450: a theoretical study of stereo-electronic modulators of product distribution. *J. Am. Chem. Soc.* **1991**, *113*, 2736–2743.

JM030608T